



HAL
open science

Predicting the steady-state infiltration rates of agricultural soils of the Mediterranean region from their soil surface conditions

Patrick Andrieux, Marc Voltz, Jean-Stéphane Bailly, Rafla Attia, Patrick Zante

► **To cite this version:**

Patrick Andrieux, Marc Voltz, Jean-Stéphane Bailly, Rafla Attia, Patrick Zante. Predicting the steady-state infiltration rates of agricultural soils of the Mediterranean region from their soil surface conditions. *Geoderma*, 2025, 461, pp.117468. <10.1016/j.geoderma.2025.117468>. <hal-05409525>

HAL Id: hal-05409525

<https://hal.inrae.fr/hal-05409525v1>

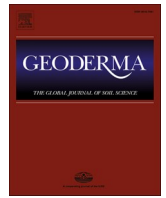
Submitted on 10 Dec 2025

HAL is a multi-disciplinary open access archive for the deposit and dissemination of scientific research documents, whether they are published or not. The documents may come from teaching and research institutions in France or abroad, or from public or private research centers.

L'archive ouverte pluridisciplinaire **HAL**, est destinée au dépôt et à la diffusion de documents scientifiques de niveau recherche, publiés ou non, émanant des établissements d'enseignement et de recherche français ou étrangers, des laboratoires publics ou privés.



Distributed under a Creative Commons CC BY 4.0 - Attribution - International License



Predicting the steady-state infiltration rates of agricultural soils of the Mediterranean region from their soil surface conditions

Patrick Andrieux^a, Marc Voltz^{a,*}, Jean-Stéphane Bailly^a, Rafla Attia^b, Patrick Zante^a

^a UMR LISAH, Univ. Montpellier, AgroParisTech, INRAE, IRD, Institut Agro, 2 Place Pierre Viala, F-34060 Montpellier, France

^b Direction des Sols, DG Acta, Tunis, Tunisia

ARTICLE INFO

Keywords:

Rainfall simulation
Classification
ANOVA
Regression tree
Crusting
Vegetation cover
Litter cover

ABSTRACT

Knowledge of soil infiltration properties is essential for managing water resources. Here, we present and evaluate an expert-based classification of soil surface conditions (SSCs) for predicting steady infiltration rates in Mediterranean soils. The classification distinguishes 9 SSC classes. To identify the SSC classes, an identification chart is proposed that uses five easy-to-observe soil surface descriptors (SSDs), namely, the soil cover percentages of clods, surface crusts, rock fragments, herbaceous vegetation and litter. To evaluate the classification, we gathered a dataset including infiltration measurements by rainfall simulations and observations of 12 different SSDs at 273 plots across southern France and Tunisia. The plots represent a range of Mediterranean crops and land uses, including vineyards, wheat, barley, chickpeas, rangeland and fallow land. The expert classification was compared with a statistically derived classification based on a regression tree approach and calibrated with the observational dataset. Variance analysis revealed that the expert SSC classification and the fitted statistical classification explained 73 % and 79 % of the variance in infiltration rates, respectively. A cross-validation test showed that the expert classification is more precise and robust than the statistical classification for predicting soil infiltration rates. The expert classification exhibited a root mean square error (RMSE) of 5.2 mm/h, much smaller than the RMSE values of current pedotransfer functions for predicting soil hydraulic conductivity. Soil surface cover characteristics, proved to be more important proxies for discriminating soil infiltration capacity than permanent topsoil properties, such as soil texture and soil types. To conclude, the expert classification provides an easy and accurate way to estimate the soil infiltration capacity of agricultural fields.

1. Introduction

Water infiltration at the soil surface is a major process influencing many other processes that are of primary importance in ecosystem functioning and human livelihood, such as groundwater recharge, soil water availability for plants, transport of solutes, soil erosion, and soil microbial activity. Knowledge of soil infiltration properties is therefore important in many regions of the world for predicting and managing the share of water resources between ecosystems and stakeholders. This is particularly the case in the Mediterranean region given the large pressure on water resources that already exists and that is expected to rise due to climate change and increasing population needs (Voltz et al., 2018). Accordingly, this paper is concerned with the prediction of the soil infiltration capacity of Mediterranean soils.

Predicting the variation in time and space of soil infiltration depends primarily on the knowledge of topsoil hydraulic properties. The methods

for measuring these properties are time-consuming and expensive, and in turn, observed data are scarce or even absent in national and international soil databases. Thus, for several decades, efforts have been made to construct databases of soil hydraulic properties from measurements (e.g., Clapp and Hornberger, 1978; Schaap et al., 2001; Tóth et al., 2017; Rahmati et al., 2018; Gupta et al., 2021) and to relate the observed values to basic soil characteristics to develop so-called pedotransfer functions (PTFs) (see reviews by Van Looy et al., 2017; Ottoni et al., 2019). For predicting soil saturated hydraulic conductivity, most of the developed PTFs apply statistical regression approaches relating basic soil properties to hydraulic conductivity (e.g., Cosby et al., 1984; Saxton et al., 1986; Vereecken et al., 1990; Wösten et al., 1999) or apply physical-empirical relationships relating particle size distribution and hydraulic conductivity using the concepts of effective porosity and effective pore radii (Van Looy et al., 2017). However, when checked on independent validation data, their performances appeared rather poor

* Corresponding author at: INRAE, UMR LISAH, 2 place Pierre Viala, 34060 Montpellier Cedex 1, France.

E-mail address: marc.voltz@inrae.fr (M. Voltz).

<https://doi.org/10.1016/j.geoderma.2025.117468>

Received 3 April 2025; Received in revised form 28 July 2025; Accepted 30 July 2025

Available online 9 August 2025

0016-7061/© 2025 The Author(s). Published by Elsevier B.V. This is an open access article under the CC BY license (<http://creativecommons.org/licenses/by/4.0/>).

(e.g., Parasuraman et al., 2006; Bormann, 2010; Groenendyk et al., 2015; Zhang et al., 2019). There are several reasons that can explain this. First, some PTFs were derived from databases that include many measurements from laboratory-scale experiments with disturbed soil samples, which are not representative of actual soil conditions. Second, the main soil properties considered as predictors in PTFs are soil texture, soil organic carbon content, bulk density and land use (Jarvis et al., 2013). These properties are indeed those that are mostly available in soil databases but do not inform on the poral structure of soils (e.g., Rahmati et al., 2018; Bargués-Tobella et al., 2024). Vereecken et al. (2019) thus advocated for the development of PTFs that consider the effects of poral structural properties on soil hydraulic conductivity. Third, infiltration properties also change with time, as influenced by changes in soil cover, soil crusting and plant rooting characteristics (Lu et al., 2020). Thus, to predict time-varying soil hydraulic properties, identifying easy-to-observe proxies that provide information on the changes in the structural properties of soils is necessary.

For topsoils, predictors of infiltration capacity can rely also on observations of soil surface descriptors (SSDs), such as soil cover, crusting, stone cover, surface roughness, etc. The SSDs may change with time according to soil treatments and land use and can be used as proxies for changes in the poral structure of topsoils. Many papers have provided evidence of the link between SSDs and topsoil infiltration or surface runoff in both natural (e.g., Descroix et al., 2001; Tighe et al., 2012) and agricultural (e.g., Berndtsson and Larson, 1987; Leonard and Andrieux, 1998; Janeau et al., 2003; Gicheru et al., 2004; Zhipeng et al., 2018) soils. Moreover, several of them proposed classifications of the soil surface conditions (SSCs) of topsoils according to the observed SSDs and related the SSC classes to the variation in the soil infiltration capacity. For example, SSC classifications were developed for soils in arid and semiarid Western Africa (Casenave and Valentin, 1992), untilled vineyard soils in southern France (Leonard and Andrieux, 1998), soils developed on loess material in northwestern France (Cerdan et al., 2001), soils from black marl landscapes of the southern French Alps (Malet et al., 2003), grazed rangelands of northern Queensland (Roth, 2004) and Chromic Luvisols in semiarid southeastern Australia (Tighe et al., 2012). These classifications are expert or statistically based. They differ strongly in the SSC classes defined and in the number and kind of SSD observations used to infer the SSC classes. The SSD observations included not only ground cover descriptors but also a range of surface and near-surface characteristics related to texture, soil structure and microtopography. Some authors have considered the near-surface characteristics over only a few centimetres from the soil surface (Cerdan et al., 2001; Malet et al., 2003; Roth, 2004; Tighe et al., 2012), whereas others have considered characteristics down to 10 or 40 cm to better analyse the influence of the soil characteristics beneath the surface on the topsoil infiltration capacity (Leonard and Andrieux, 1998; Casenave and Valentin, 1992). The differences in the latter classifications are related to differences in soils, climates, and land use occurring in the sites or areas where they were developed. The validity of these classifications is therefore limited to specific environments. To our knowledge, no SSC classification for soils in the Mediterranean region has been developed thus far.

We hypothesised that it is possible to derive such an SSC classification system on the basis of easy-to-observe SSDs and to use it for predicting infiltration capacity and its variation over time in a large range of Mediterranean agricultural soils. Accordingly, the aims of this paper are i) to present and evaluate an expert-based classification of SSC classes for predicting soil steady infiltration rates and ii) to identify the most influential SSDs for differentiating the soil infiltration capacity of Mediterranean agricultural soils.

2. An expert classification of the soil surface conditions of Mediterranean agricultural soils

The classification was developed from extensive observations over a

depth of 15 cm of the variations in the surface and structural characteristics of topsoils in farmed areas in southern France and Tunisia. Its aim was to distinguish SSC classes that correspond to the range of SSCs that can be observed in the primary Mediterranean soils and crops according to the timing of agricultural operations and crop development. The SSC classes were also meant to discriminate changes in the soil infiltration capacity and to be easy to identify in the field by simple observations or measurements. The rationale of the developed classification was based on previous work. First, the pioneering works of Boiffin (1984), Boiffin et al. (1988), Bresson and Boiffin (1990) and Valentin and Bresson (1992) distinguished several stages in the evolution of SSCs on bare arable land due to tillage and soil sealing under the impact of rainfall. In the present classification, we considered only four main stages to facilitate their recognition in the field. The first stage is just after tillage, when the structure of the topsoil has been fragmented by tillage and the soil surface is completely open without any crust. The second stage is when the first rainfalls after tillage have led to the sealing of the soil surface by a thin, continuous structural crust formed by the rearrangement of particles at the soil surface. This stage is representative of tilled soil that has received at least one significant rainfall event (Paret et al., 2011). The third stage is after a number of significant rainfall events when the topsoil both is completely closed by a structural crust and is well consolidated below the crust. The structural crust corresponds to a rearrangement without lateral displacement of the soil surface particles (Valentin and Bresson, 1992). The fourth stage is when a sedimentary crust formed instead of or above the structural crust due to sedimentation processes. This latter stage no longer changes with rainfall if no other mechanical actions occur. The first three stages can be observed frequently in Mediterranean agricultural soils after tillage, whether with annual crops or perennial crops such as vineyards. The fourth stage is less frequent because its development is slow and often hindered by biological activity and tillage. Second, several works have shown the major influence of soil cover by vegetation, litter and rock fragments on soil surface infiltration properties (e.g., Poesen et al., 1990; Poesen and Lavee, 1994; Thompson et al., 2010; Wang et al., 2020; Zi et al., 2024). Accordingly, the present classification considers not only the tillage and soil sealing effects of rainfall but also the additional influence of soil cover characteristics on soil infiltration.

Overall, the classification distinguishes 9 SSC classes (Fig. 1). They are described hereafter:

T: This is the SSC class that is generated by tillage, which loosens the topsoil structure and increases soil porosity. In the field, this SSC is recognised by the fragmentary structure of the soil surface, which clearly features identifiable clods, marked roughness and overall weak consolidation of the topsoil. Owing to tillage, no surface sealing or vegetation presence can be observed, and only coarse elements or stones may be observed following the stoniness of the topsoil.

TCst: This SSC class follows the previous SSC T when the first rainfall events have occurred after tillage. The topsoil consolidation is still weak, but a thin structural crust, a few millimetres thick, has formed on at least part of the soil surface under the influence of raindrops. For this SSC class, the structure of the soil beneath the crust is slightly modified compared with that of T. In the field, TCst can be recognised by a high surface roughness and the presence of clods under the crusted part of the soil surface. Herbaceous vegetation and litter may begin to appear, but they cover less than 50 % of the surface.

Cst: This SSC class occurs when the impact of raindrops has led to the development of a continuous structural crust on the surface of the soil, regardless of whether it has been tilled previously. This SSC class is identified by a completely closed soil surface with a consolidated crust and no visible clods. The soil surface is bare or has very little vegetation or litter cover. The soil consolidation below the crust is generally strong even if the soil was previously tilled.

Csd: This SSC class differs from Cst in terms of the type of surface crust, which is now sedimentary (also referred to as depositional; see Valentin and Bresson, 1992). The formation of a sedimentary crust

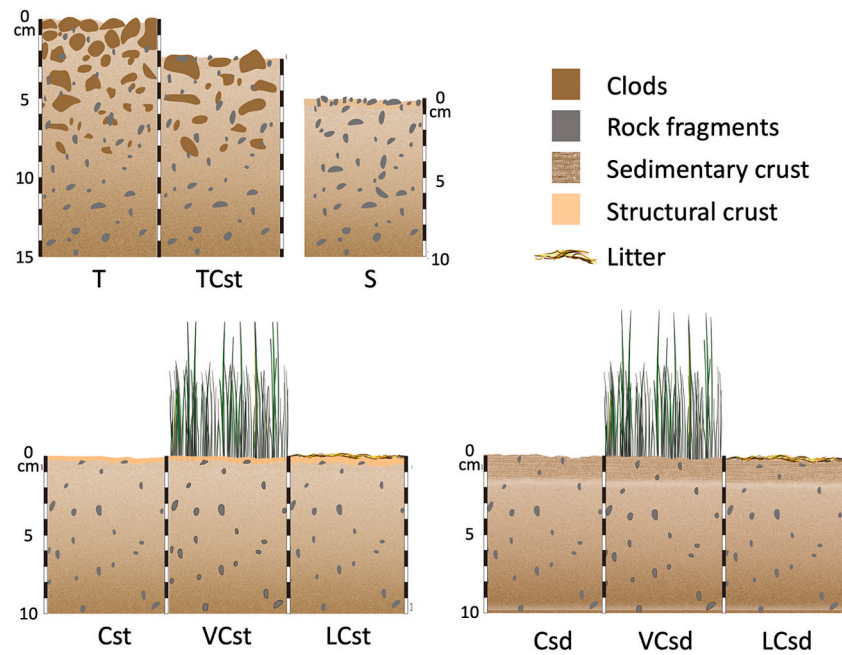


Fig. 1. The 9 soil surface condition classes of the expert-based SSC classification.

generally but not always follows that of a structural crust during the process of sedimentation of suspended matter from low runoff or stagnant water at the soil surface that occurs at the end of runoff events. The sedimentary crust consists of several layers of successive deposits, varying in thickness up to several centimetres. It may overcome an initial structural crust. As with Cst, the soil is well consolidated under the crust. In the field, this SSC can be recognised by a smooth, low-roughness surface and a crust with a bedded structure, often with layers of coarse particles towards the bottom and finer particles towards the top. As with Cst, no clods are observed on the soil surface, which is bare or has low vegetation and litter cover.

VCst and LCst: These two SSC classes correspond to specific cases of Cst where either herbaceous vegetation or plant litter or debris cover more than 50 % of the soil surface. VCst and LCst are recognised via the same criteria as those for Cst, to which the criterion of a soil cover of more than 50 % by vegetation or litter is added.

VCsd and TCsd: These SSC classes correspond to specific cases of Csd where either herbaceous vegetation or plant litter or debris cover more than 50 % of the soil surface. VCsd and LCsd are recognised via the same criteria as those for Csd, to which the criterion of a soil cover of more than 50 % by vegetation or litter is added.

S: This SSC class corresponds to the specific case of very stony soils where the soil is covered by more than 50 % by rock fragments. The topsoil exhibits overall strong consolidation with no observable clods. In these very stony soils, a structural or sedimentary crust may be present but not dominant, and tillage does not produce significant amounts of clods.

To identify the SSC classes according to the expert classification, an identification chart was developed based on five qualitative SSDs that are easy to observe in the field:

- Percentage of surface cover by soil clods exceeding or not exceeding 25 %
- Percentage of surface cover by rock fragments exceeding or not exceeding 50 %
- Percentage of surface cover by herbaceous vegetation exceeding or not exceeding 50 %
- Percentage of surface cover by litter or plant debris exceeding or not exceeding 50 %

- Major crust type when present: structural or sedimentary

For simplicity, the structure of the identification chart was chosen to be dichotomous with as many levels of split as SSDs (Fig. 2). The hierarchy of the descriptors in the chart was defined to identify successively the SSC classes influenced by tillage, rock fragments, vegetation, litter and, eventually, crust. For soil clods, the critical threshold was considered to be 25 % only because even a limited soil cover by clods clearly indicated that the SSC class was either T or TCst. In accordance with the observations of Poesen et al. (1990), Neave and Rayburg (2007), Ruiz Sinoga et al. (2010) and Tighe et al. (2012), the average threshold of 50 % coverage was chosen for rock fragments, herbaceous vegetation and litter as a critical value at which marked changes in the soil infiltration capacity occur.

3. Material and methods

3.1. Study sites and sampling

The observations and measurements used in this paper were gathered from both a set of infiltration experiments under simulated rainfall and SSD observations carried out as part of several experimental campaigns that aimed to identify the pedological and agronomic factors affecting the variability of infiltration in Mediterranean soils. The experiments took place from 1993 to 2003 at two study sites in southern France, Roujan (43.489°N/03.315°E, Leonard and Andrieux (1998)) and Puisseguier (43.378°N/03.046°E, Andrieux et al. (2007)), and from 2004 to 2008, at three study sites in Tunisia, Kamech (36.875°N/10.876°E, Zante et al. (2009)), El Gouazine (35.898°N/09.697°E, Zante et al. (2007)) and El Hnach (36.069°N/09.448°E, Attia et al. (2009)) (Fig. 3). At the first three sites, the climate is subhumid Mediterranean with similar average annual rainfall of approximately 650 mm, whereas at the latter two sites, the climate is semiarid, with average annual rainfall varying between 395 and 470 mm. The observations were made on 1 m² subplots distributed within 60 different field plots among the five study sites. The number of subplots per field plot varied from 1 to 5 depending on the variability of the SSC classes identified within each field plot during the growing season. In total, 273 subplots were measured. This observation design allowed the sampling of a wide range

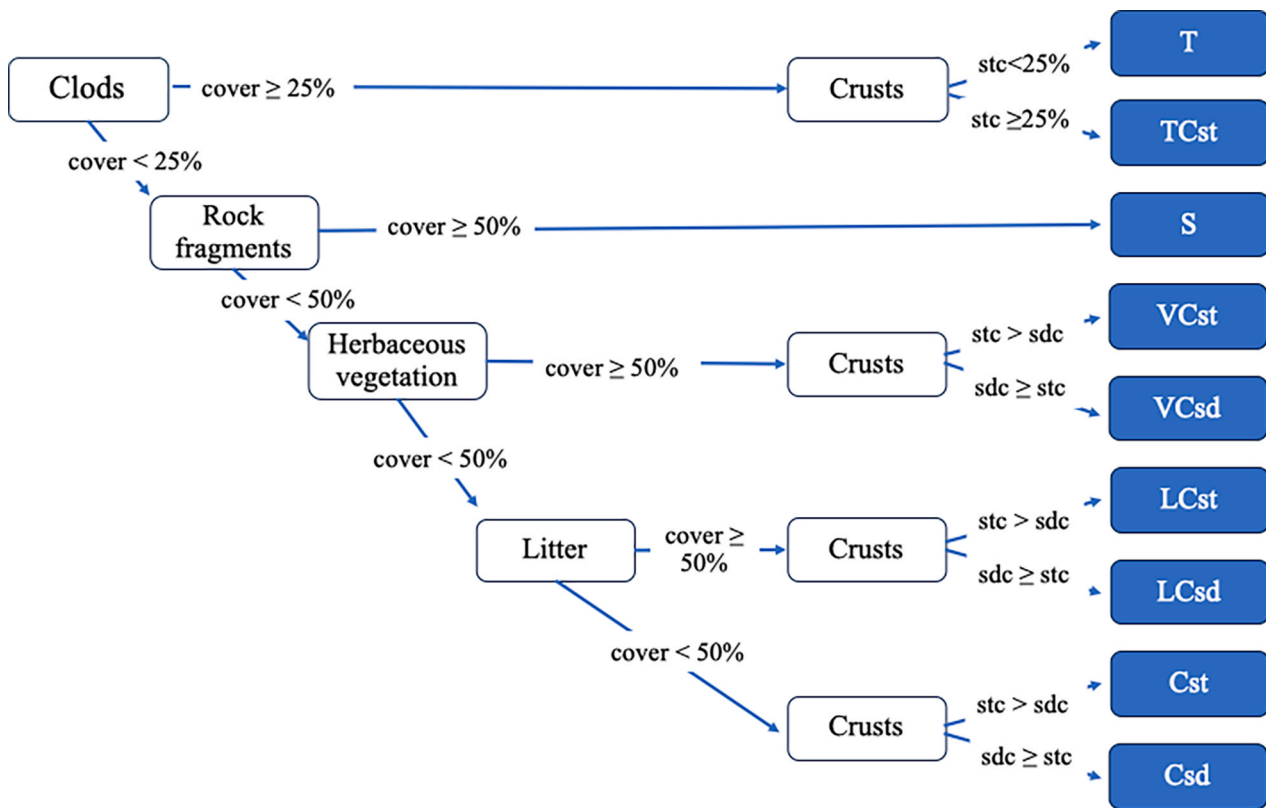


Fig. 2. Identification chart of the expert-based SSC classes. Acronyms “sdc” and “stc” mean “sedimentary crust” and “structural crust”, respectively.

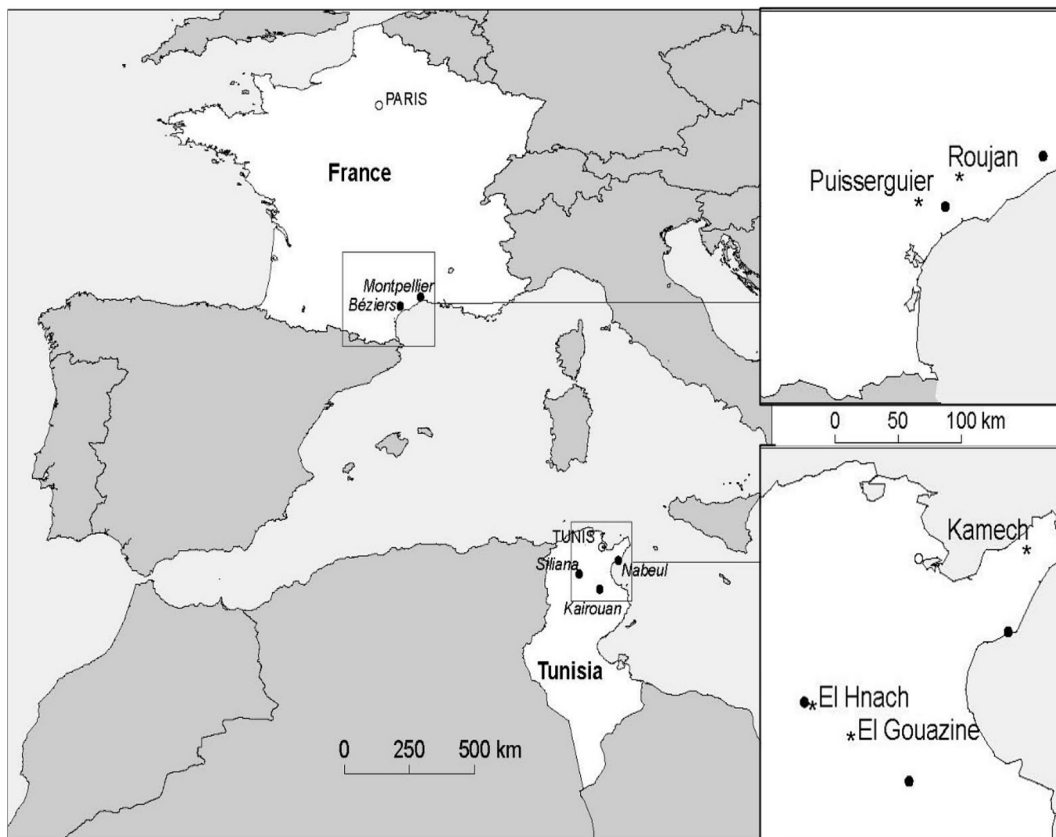


Fig. 3. Location of the study areas and sites: Roujan, Puisserguier, Kamech, El Hnach, El Gouazine.

of soils and land uses, representative of those found in Mediterranean farmed environments (Table 1). Six soil types were distinguished among the studied plots, including four calcareous and two noncalcareous soils. According to the WRB-FAO soil classification (IUSS Working Group WRB, 2015), they consist of calcareous Leptosols, Calcisols, vertic Calcisols, and calcareous Cambisols for calcareous soils and vertic Leptosols and vertic Cambisols for noncalcareous soils. These soils cover large areas in the cultivated Mediterranean zone and represent most of the soil classes observed in the Mediterranean area (European Soil Bureau Network, 2005; European Environment Agency, 2012), with the exception of Luvisols. Moreover, they cover a large range of textures, with clay contents ranging from 5–64 %, silt contents ranging from 3–70 % and sand contents ranging from 13–83 % (Fig. 4). The surface organic carbon content in the 0–20 cm surface layer varies from 0.2–2 % among the 60 field plots, which is typical of the usually low organic carbon content of farmed Mediterranean soils (Lagacherie et al., 2018). The land uses sampled at the five sites are also typical of the range of land uses found around the Mediterranean, namely, perennial crops, such as vineyards (*Vitis vinefera*); annual crops, such as wheat (*Triticum aestivum* and *durum*), barley (*Hordeum vulgare*) and chickpea (*Cicer arietinum*); and grazing land and fallow land. The subplots within the field plots were chosen to represent the major SSC classes that each type of land use generates either spatially at a given time or over time in relation to climate, vegetation development or soil management. In vineyards, the SSCs are strongly influenced by the succession of soil maintenance operations, which influences the presence or absence of crusts on the soil surface, changes in soil pore structure and grass development (Leonard and Andrieux, 1998; Biarnes et al., 2004; Pare et al. 2011; Morvan et al., 2014). A preliminary survey identified three main types of soil treatments of vineyards that lead to different sequences of SSC classes. In the first one, chemical weeding is performed over the whole field without any tillage. Consequently, the SSCs remain the same throughout the year. In the other two treatments, herbicides are applied only along the vine rows, whereas the inter-rows are tilled one to four times per year or covered permanently with grass. In these last two soil treatments, the SSCs vary with time due to tillage or changes in the extent of grass cover. The locations and observation dates of the subplots within the vineyard plots were chosen to sample the SSCs immediately after the cultivation operations and at various times when significant changes can be observed either in the soil structure in connection with surface crusting processes or in grass cover. For annual crops, the SSCs are influenced mainly by soil preparation for the seedbed, the development of vegetation after sowing and harvesting, which leaves a stubble that is grazed in some cases. The subplots were therefore chosen to observe the differences in SSCs and steady-state infiltration rates at these three stages. For rangeland and fallow land, the SSCs are assumed to be stable over time. The soils are often stony and/or have more or less scattered plant cover. In all, among the 273 subplots, 75 are vineyards, 157 are arable cropland and 41 are rangeland or fallow land.

Table 1
Number of observed plots and sub-plots per land use and soil types. (C) and (NC) stand for “calcareous” and “non calcareous” soils.

		Plots	Subplots
Land use	Vine	42	75
	Wheat and barley	10	135
	Chickpea	2	22
	Rangeland	3	12
	Fallow land	3	29
Soil	Calcareous Leptosol (C)	5	43
	Calcisol (C)	33	99
	Vertic Calcisol (C)	3	35
	Calcareous Cambisol (C)	15	49
	Vertic Leptosol (NC)	1	9
	Vertic Cambisol (NC)	3	38
Total		60	273

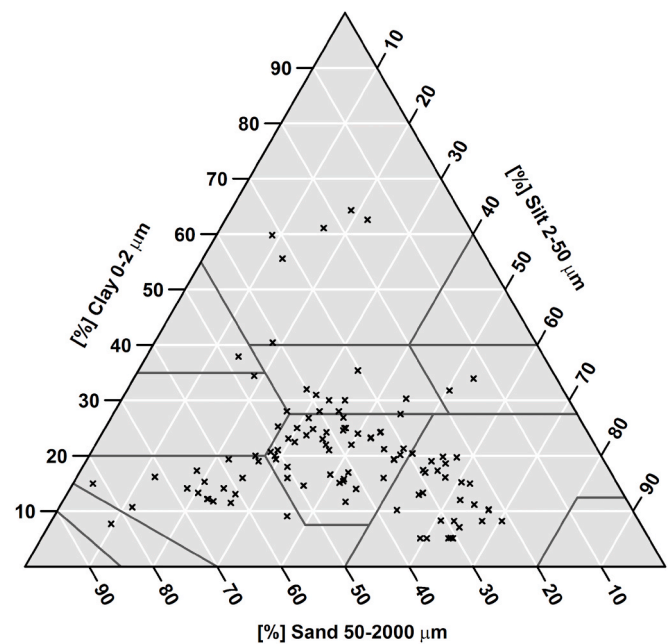


Fig. 4. Variation of topsoil texture among the sampled field plots according to FAO texture triangle.

3.2. Measurements

3.2.1. Steady-state infiltration rates estimated via rainfall simulations

A field oscillating rainfall simulator, which is based on the design of Asseline and Valentin (1978) and Casenave and Valentin (1992), was used to apply rainfall to a 10 m² area. A metal runoff frame 1 m by 1 m in size was inserted approximately 10 cm into the soil in the centre of the rainfall area. The runoff frame was connected with a trough placed downhill to collect surface runoff. Rainfall simulation was performed over a 10 m² area including the 1 m² frame to favour one-dimensional infiltration over the frame and avoid boundary effects on the determination of surface runoff from the frame. Rainfall was applied at a height of 4.30 m above the ground at a mean rate of 35 mm/h (in a range between 33 and 43 mm/h) until surface runoff became constant, which occurred in all the experiments between 30 and 60 min after the start of rainfall. The rainfall intensity from the simulator was calibrated before each rainfall simulation by measuring surface runoff on an impermeable 1 m² pan placed over the runoff frame and by selecting an adequate angle of nozzle oscillation. Runoff rates were measured by taking volumetric samples of the water discharged from the trough at the outlet of the metal frame. The steady-state infiltration rate (*i_s*) was estimated by the difference between the controlled rainfall intensity and the recorded runoff rate when surface runoff reached a plateau. Importantly, the infiltration rates measured by rainfall simulations were intrinsically limited by the applied rainfall intensity, i.e., 35 mm/h in our simulations.

3.2.2. Observation of soil surface descriptors

In all plots and subplots, 12 SSDs were observed, which have already been shown in the literature to be proxies of the variation in the partitioning of rainfall into surface runoff and soil infiltration (e.g., Gysse and Poesen, 2003; Le Bissonnais et al., 2005; Arnau-Rosalén et al., 2008; Tighe et al., 2012), and whose observations can be kept simple. The 12 SSDs included all criteria of the identification chart of the expert classification for identifying the major SSC class of each subplot. They consisted of soil texture as defined by clay, silt and sand contents; slope; topsoil consolidation; surface roughness; and percentages of soil cover by coarse elements, clods, structural and sedimentary crusts, herbaceous vegetation and litter. Most of the latter variables are quantitative and are

expressed as areal or mass percentages. Only surface roughness and topsoil consolidation were estimated on a categorical scale.

A detailed presentation of the observation or measurement techniques is given in the summary reports of the various experiments. Here, we summarise only the main features of the observation methods, most of which, apart from the measurement of soil texture, were chosen to be easy to apply by a field surveyor with moderate experience.

The **topsoil clay** (0–2 μm), **silt** (2–50 μm), and **sand** (50–2000 μm) contents were measured at the INRAE Soil Laboratory in Arras (France) by the standard sedimentation and sieving methods (AFNOR, 2003) on air-dried samples taken from the 0–5 cm soil layer.

Topsoil consolidation was estimated in order to distinguish between subplots that were recently tilled and those that were not. Recently tilled soils exhibit an unconsolidated structure with a loose arrangement of soil clods and aggregates and low bulk density whereas not tilled or formerly tilled soils exhibit most often a consolidated structure with higher bulk density (Sandin et al., 2018). Topsoil consolidation was judged on micro soil profiles that were dug across the 0–15 cm soil layer after each rainfall simulation trial by observing the morphological structure of the soil and by pushing a knife in the soil to evaluate its penetration resistance. Given the highly qualitative nature of these observations, topsoil consolidation was classified roughly as weak or strong.

The **slope** of each subplot was measured manually over a distance of 2 m with a line level.

The **surface roughness** was defined as in Ludwig et al. (1995). Roughness is estimated by the difference in the heights of the deepest part of the microdepressions and the lowest point of their rim. Compared with Ludwig et al., we considered only 3 roughness classes instead of 5, namely, R0 (low, 0–2 cm), R1 (medium, 2–5 cm) and R2 (high, ≥ 5 cm). The latter three classes correspond to the roughness values generated by the three main tillage tools observed at our study sites: 1 to 2 cm for the horizontal rotary cultivator, 2 to 5 cm for the tine cultivator and more than 5 cm for the plough.

The **percentages of soil cover by rock fragments, clods, structural and sedimentary crusts, herbaceous vegetation and litter** were estimated by the quadrat method with square frames of 1 m² subdivided in 10 cm x 10 cm squares, which are frequently used for vegetation inventories. The estimated accuracy of these measurements was 5 %. The sum of all cover variables apart from herbaceous vegetation was kept at 100 %. Herbaceous vegetation includes grass and short crops, such as wheat, barley and chickpea. Rock fragments were considered when their size was larger than 2 cm, which corresponds to fragments equal to or larger than coarse gravel according to FAO guidelines for soil

description (Fig. 5 page 30 in FAO (2006)).

3.3. Evaluation of the SSC expert classification

The SSC expert classification was assessed in four steps. First, we evaluated whether the SSC classes effectively explained the variation in the soil steady-state infiltration rates. We performed a one-way ANOVA to confirm an overall significant difference between the class means of soil infiltration rates and to estimate the variance in infiltration rates explained by the expert classification. Given the heteroscedasticity of variances between SSCs indicated by Levene's test, we performed Welch's unequal-variance *t* test to test the significance of the ANOVA model. Second, we ran Tukey's pairwise post hoc test to assess which SSC classes were significantly different from one another in terms of infiltration rates. Third, we compared the SSC expert classification for predicting infiltration rates to a direct statistical clustering model that links all the soil surface descriptors and the observed infiltration data. For that purpose, a classification and regression tree or CART model (Breiman et al., 1984) was trained on the same database as the one used for evaluating the expert clustering (12 soil surface descriptors, 273 individuals). The CART process involves the design of an explicit and easily interpretable hierarchical key starting from soil descriptors and targeting the best prediction of infiltration rate variations. The tree pruning process in CART was performed using default rules (among other rules, the process stopped if, at a step, the overall R-squared increased by less than 1 % or if a node had fewer than 20 individuals), as proposed by Breiman et al. (1984) and implemented within the Rpart R programming package (Therneau et al., 2013). The importance of each of the variables selected by CART for splitting groups of data was computed by the sum of the differences in residual sum of squares (RSS) at all tree splits where that variable is used as a main or surrogate splitting variable (see for more details Breiman et al., 1984). Finally, a cross-validation approach was operated to test the classifications' ability to predict infiltration rates of plots not used for calibrating the mean infiltration rates of the SSC classes. The approach consisted in running 100 times a K-fold cross-validation, with $K = 10$ as recommended by Hastie et al. (2001). The idea of K-fold cross validation is to randomly divide the initial data into K equal-sized parts, namely here 10 random sets of 10 % of the data, and for each K part to train the classifications on the remaining data, namely 90 % of the data, and then to obtain predictions for the K part. In all the cross-validation approach allowed to get for each classification 1000 performance estimates from which we computed its average RMSE value.

4. Results

4.1. Variation in the SSC classes between the observation plots

As expected, the diversity of the SSC classes depends on the type of land use (Fig. 5). Vineyards exhibit all of the classes. They are almost the only land use for which the SSC classes with a marked presence of sedimentary crusts are observed, which has to be related to the long period of bare soil and no tillage practices that are experienced by some vineyards in the Mediterranean area. Annual crops essentially exhibit a sequence of SSC classes from the tilled SSC class to the classes with marked structural crusts. Indeed, sedimentary crusts are less likely to develop on annual crops where the soil is most often subjected to some kind of tillage once a year and does not remain bare over a sufficiently long period. The SSC classes related to significant vegetation or litter cover concern all land uses except rangeland, whose vegetation is regularly grazed and remains sparse throughout the year in Mediterranean areas. The SSC class S only concerns vineyards, rangeland and fallow land, which is consistent with the fact that stony soils are much more devoted to these land uses than to annual crops.

The values of SSDs are, in most instances, well in line with the SSC classes on which they were measured (see Fig. SM1). This is by

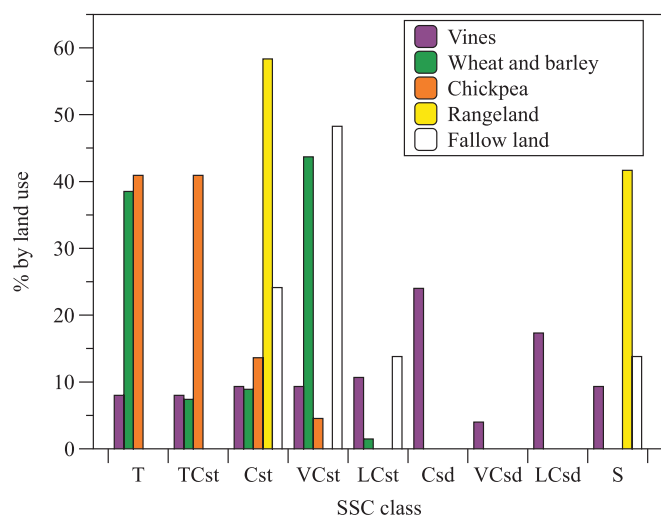


Fig. 5. Distribution of expert-based SSC classes among each land use.

construction because the six soil cover descriptors were used as classification criteria. But it is also so for topsoil consolidation that switches from weak to strong from the first two SSC classes, T and TCst that occur just after tillage, to the SSC classes exhibiting structural and sedimentary soil crusts. Roughness also decreases across the same sequence; however, some high values of roughness exist for SSC classes that combine a structural crust and vegetation or litter cover. In terms of soil texture, there are some variations among the SSC classes. The classes exhibiting sedimentary crusts Csd, VCsd and LCsd do not include very clayey or sandy topsoils, in contrast to the other classes apart from the S class. This may be related to the fact that these classes are only observed on vine plots that exhibit medium textures (see Table SM2). Finally, it is worth noting that there are no marked differences in the distributions of slope values between the various SSC classes.

4.2. Variation in infiltration rates between the SSC classes

The steady-state infiltration rates range from 1.9–36 mm/h. Two groups of SSC classes can be distinguished with respect to infiltration rates (Fig. 6). The first group consists of the SSC classes T, TCst, VCst, LCst and S, which exhibit infiltration rates higher than 20 mm/h. These SSCs classes correspond to topsoils that were either subjected to recent tillage practices that increased soil porosity or were covered by vegetation, litter or rock fragments that counterbalanced the effect of soil sealing by structural crusts or prevented soil sealing. The second group consists of the SSC classes Cst, Csd, VCsd and LCsd, whose infiltration rates are most often lower than 20 mm/h. All the latter SSCs exhibit soil sealing that decreases the soil infiltration capacity, which is only slightly improved by vegetation and litter cover in the case of soil sealing by a sedimentary crust. Finally, it is worth acknowledging that the observed infiltration rates are limited by the rainfall simulation intensity of 35 mm/h. Consequently, it is likely that the maximum measured rates are lower than the maximum actual rates. Accordingly, the means and ranges of the infiltration rates of the SSC classes T and VCst, with values close to 35 mm/h, are certainly underestimated.

4.3. Correlation between infiltration rates and SSDs

The graphs between the infiltration rates and all SSDs in Fig. 7 show that no single SSD can explain the infiltration rate variation across all subplots. Three major types of relationships can, however, be noted. For clay content, slope and structural crust cover, there is almost no change

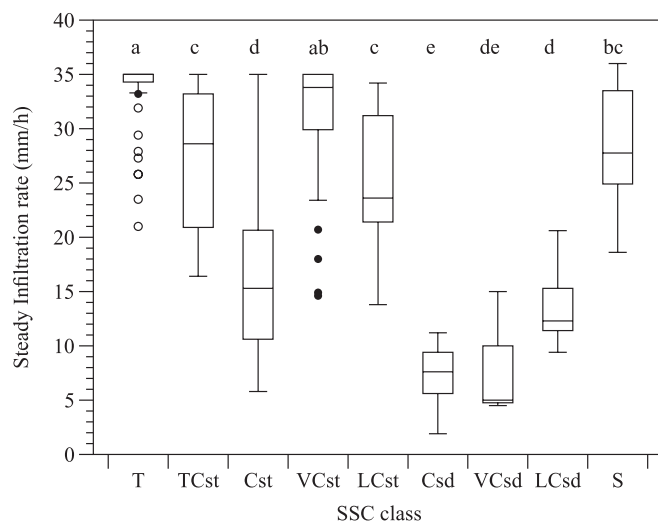


Fig. 6. Box-plots of steady infiltration rates per expert-based SSC class. According to the Tukey's pair wise post-hoc test, SSC classes with different letters exhibit significant differences in mean infiltration rates with p-values less than 0.05 while SSC classes sharing same letters do not.

in the range of observed infiltration rates with varying values of these SSDs. For sedimentary crust cover, there is a very marked and progressive narrowing of the range of infiltration rates towards lower rates with increasing soil cover, which demonstrates the negative impact of sedimentary crust development on the soil infiltration capacity. Finally, the other SSDs show a more or less noticeable narrowing of the range of infiltration rates towards higher values when the SSD value increases. It is clear and progressive for roughness class, rock fragment cover, clod cover, and vegetation cover, whereas it is limited for soil consolidation and litter cover or starts only above a threshold for the silt and sand contents, namely, 60 % and 50 %, respectively.

4.4. Predicting soil steady-state infiltration rates by the expert SSC classification

The variance analysis reveals that, on average, there is a highly significant difference in the mean infiltration rates among the expert SSC classes at a probability level less than 0.001 (Table 2). The ratio of the between expert SSC classes and the total sum of squares in Table 2 is 0.073 which means that the percentage of infiltration rates explained by the SSCs is 73 %. The prediction of topsoil steady infiltration rates by the mean rates of the expert SSC class exhibits a very stable performance among the 100 runs of 10-fold cross-validations because the RMSE values range from 5.1–5.3 mm/h, with an average of 5.2 mm/h.

The results of Tukey's pairwise post hoc tests provide insight into whether pairs of SSC classes are significantly different from each other in terms of the mean infiltration rates (see the letters in Fig. 6). In this respect, we can grossly divide the 9 SSC classes into 4 main groups, including SSCs that are not significantly different. In decreasing order of infiltration rates, the four groups are (1) T and VCst (letters a and ab); (2) TCst, LCst, and ST (letters bc and c); (3) Cst and LCsd (letter d); and (4) Csd and VCsd (letters e and de). Apart from group (4), which includes two SSC classes with sedimentary crust cover, the other three groups are not consistent in terms of SSCs because they include SSCs whose characteristics differ greatly. Moreover, some SSC classes are in between these four groups. Consequently, there is no obvious grouping between SSCs that can simplify the expert classification in a consistent way without decreasing the performance of the classification for predicting infiltration rates.

4.5. Predicting soil steady-state infiltration rates by statistical SSC classification

When the whole dataset is used, the statistical clustering of SSDs by CART to achieve the best prediction of infiltration rates is shown in Fig. 8. The outcome is 11 different SSC classes, which explain 79 % of the infiltration rate variance as estimated by ANOVA (Table 2). The variance explained by CART classification is thus only slightly better than that of the expert classification, although the CART classification was fitted to the infiltration data, whereas the expert classification was not. In addition, the cross-validation runs reveal that the RMSE of the CART classification ranges from 5.5–6.2 mm/h, with an average value of 5.8 mm/h. This finding indicates that the performances of the fitted CART classifications are not only less precise on average than those of the expert classification but also less robust for predicting infiltration rates of Mediterranean agricultural soils. The criteria used by CART to discriminate between the SSC classes include the SSDs already used by the expert classification, namely, the percentages of soil cover by clods, stones, vegetation, litter and structural and sedimentary crusts. They also include three additional SSDs, silt and sand contents and slopes. The splitting thresholds for the criteria are quite different between the two SSC classifications. In the expert classification, they are fixed at 25 % for clod cover and at 50 % for the other SSDs, whereas in the CART classification, thresholds are set at 38 % for clod cover, which is not too far from the expert value, but vary from 4–59 % for the other soil cover descriptors. Therefore, by choosing a threshold of 50 % for all but one

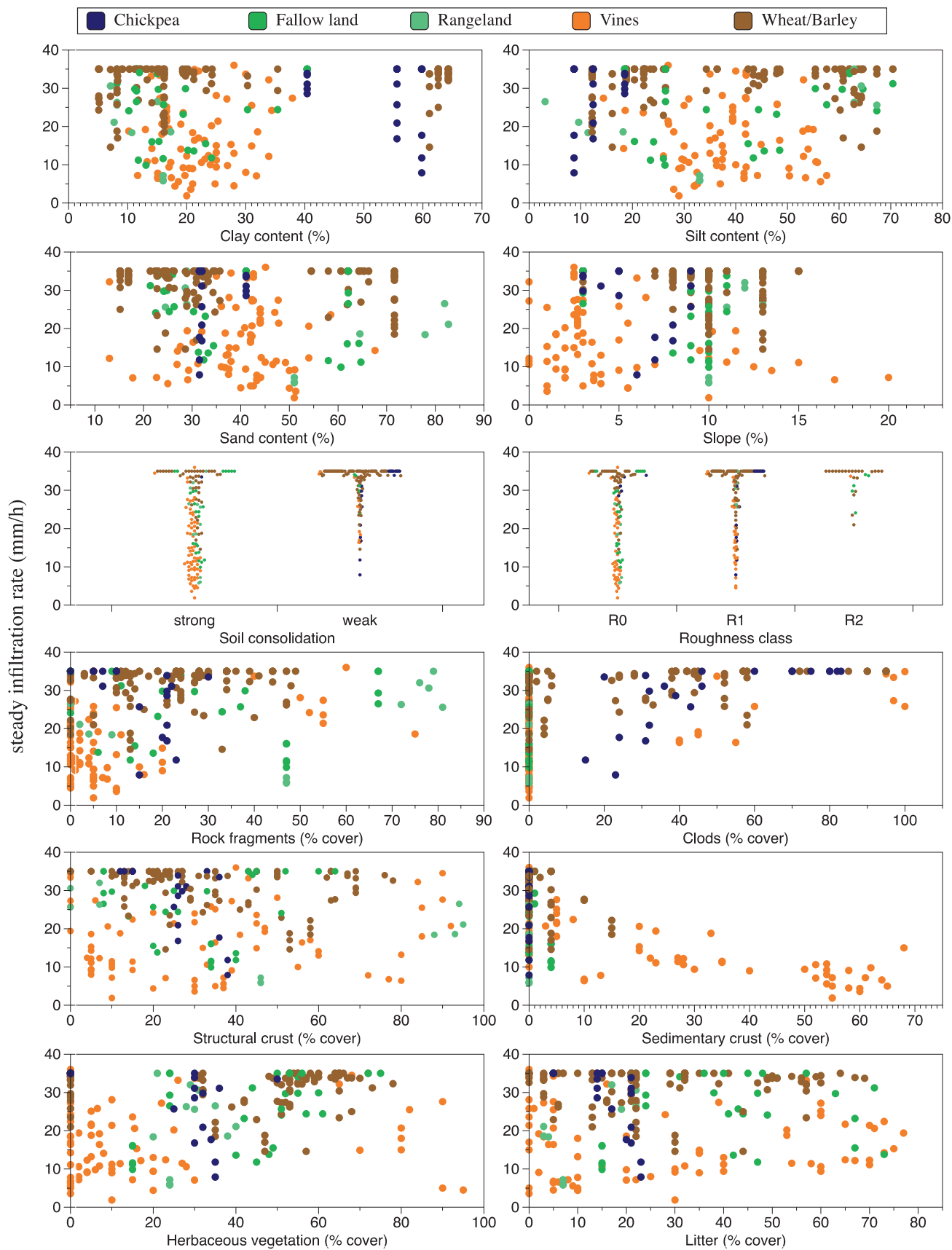


Fig. 7. Observed steady infiltration rates as a function of soil surface descriptors.

Table 2
Analysis of variance of the infiltration rates with SSC classes of the expert-based and CART SSC classifications.

	Source of Variance	Degrees of freedom	Sum of squares	Mean square	F value	p-value
Expert-based SSC classification	Between SSC classes	8	18,880	2360.0	88.7	<2e-16
	Within SSC classes	264	7024	26.6		
	Total	272	25,904			
CART SSC Classification	Between SSC classes	10	20,434	2043.4	97.86	<2e-16
	Within SSC classes	262	5470	20.9		
	Total	272	25,984			

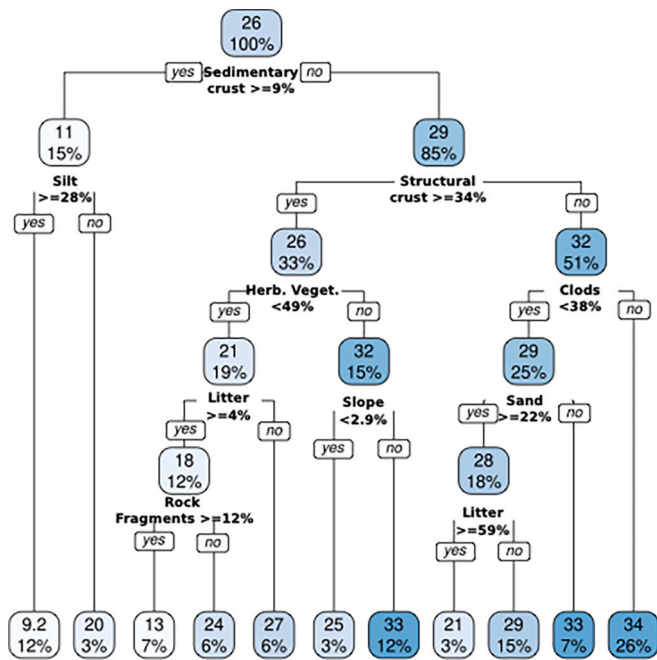


Fig. 8. CART regression tree for predicting topsoil steady infiltration rates from soil surface descriptors. The boxes with blue background represent the data subset. The numbers in each box are the mean infiltration rate in mm/h of the subset and the percentage of the subset within the full dataset. Below each box are the rules fixed by CART to split the subsets.

cover descriptor, the expert classification may underestimate, on average, the influence of increasing soil cover by most SSDs in comparison with the CART classification.

5. Discussion

5.1. Prediction performance of soil infiltration by SSC classifications

Only a few papers have explicitly considered SSC classes for quantitatively predicting the hydraulic properties of topsoils (Tongway and Hindley, 1995; Leonard and Andrieux, 1998; Cerdan et al., 2001). Our study is in line with these papers. Our findings indicate that SSC classification can accurately discriminate the steady-state infiltration rates of agricultural Mediterranean soils and can be used as a class PTF to predict the steady-state infiltration rate of a plot. The accuracy of the predictions is very satisfactory, with an RMSE of 5.2 mm/h (which corresponds to an RMSEs of 0.12 for $\log(i_s)$ predictions). These RMSE values are 2 to 10 times lower than those of classical PTFs developed for predicting saturated hydraulic conductivity (K_s), which exhibits in principle similar variation than i_s . For example, the PTFs developed by Toth et al. (2015) for $\log(K_s)$ predictions of European soils exhibit RMSEs values ranging from 0.9 to 1.36 whereas the PTFs of Zhang and Schaap (2017) developed for North American and European soils and the PTFs of Ottoni et al. (2019) derived for Brazilian and European soils have RMSEs values greater than 0.58 and 0.66, respectively. A recent

machine learning-based PTF derived for US soils (Pham and Won, 2022) showed a better RMSE value, but it was still up to 0.282. This difference in accuracy between these K_s PTFs and our expert-based class PTF for steady infiltration rates may be related first to the difference in measurement area or volume of the data used. Indeed, most classical PTFs are based on data observed on sample volumes with characteristic lengths smaller than 10 cm, whereas the infiltration rates used in this study were measured over a 1 m² area, which means that the former data are intrinsically more variable and less predictable than the latter data because of a lower degree of integration of the local soil pore heterogeneity. However, the difference in accuracy may also be a confirmation that using SSC classes as predictors conveys more relevant information on the poral structural properties of topsoils than the predictors used by the classical PTF approaches do. Recent PTF approaches have also progressively considered other proxies of soil pore structure, such as total porosity, effective porosity, and macroporosity (e.g., Tóth et al., 2017; Jorda et al., 2015; Ottoni et al., 2019; Aguilera et al., 2022; Bargués-Tobella et al., 2024), and other potential predictors, such as soil chemical properties, land use and management, vegetation cover or climate (e.g., Tóth et al., 2017; Jorda et al., 2015; Ottoni et al., 2019; Aguilera et al., 2022; Bargués-Tobella et al., 2024; Blanchy et al., 2024). Among these latter proxies, land use and vegetation cover have been shown to significantly improve the K_s prediction performance (Jorda et al., 2015; Aguilera et al., 2022; Bargués-Tobella et al., 2024; Blanchy et al., 2023), which illustrates the influence of land management on K_s . Owing to the good performance of our SSC classification, it comes that combining land use classes with descriptors or proxies of soil surface cover and soil surface state may improve prediction of the soil hydraulic properties. Moreover, synthesizing all land use and SSC information into SSC classes allows us to handle the intrinsic multidimensional nonlinear correlations of all the predictors and their nonlinear relationships with the soil infiltration capacity.

5.2. Influential SSDs for discriminating soil infiltration

Identifying SSDs that can effectively discriminate soil infiltration capacity and, more generally, the hydrological properties of topsoils has been the subject of a number of papers. There is no unique answer because it depends on the intrinsic variability and hydrological processes present in the studied soil systems. For Mediterranean soils, it is possible to rank the 12 SSDs that were observed in this study in three categories: those selected by both classifications, those selected by one only and those not selected by any.

The first category includes all SSDs considered by the expert classification because they are also selected by the CART classification, namely, all soil cover characteristics, crusts, stones, clods, vegetation and litter. Each of them exhibits some relationship with infiltration rates (Fig. 7). All of these factors, apart from clod cover, have already been recognised in previous studies to influence or inform topsoil infiltration properties. Soil crusting is well known to reduce the soil infiltration capacity and increase runoff (e.g., Assouline, 2004; Chahinian et al., 2006b; Neave and Rayburg, 2007; Yang et al., 2016). Accordingly, the occurrence of crust types has already been used for discriminating soil infiltration capacity and runoff generation (Casenave and Valentin, 1992; Cerdan et al., 2001; Malet et al., 2003; Arnau-Rosalén et al.,

2008). In this study, the expert SSC classification considers that each crust type, sedimentary or structural, is a discriminating criterion of similar importance, whereas the CART classification provides a hierarchy between the two crust types, considering that sedimentary crust cover has a greater discriminating influence than structural crust cover (Table SM4). Because the CART classification is inferred from the infiltration data, it illustrates the more pronounced effect of sedimentary crusts on infiltration rates than that of structural crusts, which can be seen in Fig. 7. Sedimentary crusts have an apparent effect on infiltration as soon as they cover more than 9 % of the soil surface. In contrast to soil crusting, other soil surface descriptors, such as rock fragments, living vegetation, and litter, are generally considered to favour soil infiltration capacity by protecting the soil surface from raindrop impact and thereby from soil crusting (e.g., Poesen et al., 1990; Cerdà, 2001; Martínez-Zavala et al., 2008; Arnau-Rosalén et al., 2008; Zi et al., 2024 for rock fragment influence; Thompson et al., 2010; Shao and Baumgartl, 2014; Vereecken et al., 2019 for vegetation cover influence and Wang et al., 2020 for litter cover influence). Furthermore, living vegetation is also expected to permeate the soil (Vereecken et al., 2019). Indeed, positive relationships are observed between rock fragment, vegetation and litter cover rates and steady infiltration rates (Fig. 7). The negative relationships of rock fragment and litter cover rates with soil crust cover (see Fig. SM3) suggest that, as expected, their main positive impact on soil infiltration is the protection of the soil against soil sealing. However, for herbaceous vegetation cover, surprisingly, no negative relationship is detected with soil crust cover (Fig SM3). Therefore, it may be speculated that the major positive effect of herbaceous vegetation on soil infiltration is not soil protection from rainfall impact but rather a rooting effect because root development enhances soil macroporosity and roots break through any existing surface crust. This would, however, require a more comprehensive investigation because our analysis merged vegetation cover data stemming from very different kinds of vegetation and soil treatments. The clod cover percentage, which has never been considered in earlier studies as a discriminating SSD for infiltration, appears to be a significant criterion for discriminating infiltration rates. Indeed, the soil clods formed by tillage practices slowly break down and slake under the influence of raindrop impact, which decreases both surface roughness and soil porosity (see Mwendera and Feyen, 1994); in turn, their disappearance at the soil surface is a proxy for the known decrease in the soil infiltration capacity after tillage (Chahinian et al., 2006a).

The second category of SSDs includes slope, silt and sand contents, which are selected as discriminating variables in the CART classification only. Slope is often cited as a factor of topsoil infiltration (e.g., Essig et al., 2009; Morbidelli et al., 2018), but its exact role, as observed by in situ measurements, is still not clear because the slope factor is often influenced by confounding factors (see review by Morbidelli et al., 2018). Soil texture is evidently a main factor generally considered in the prediction of soil hydraulic properties, but as mentioned above, it is not sufficient per se given the importance of other factors (e.g., Jarvis et al., 2013; Blanchy et al., 2023). Here, despite the large range of soil textures among the sample plots, soil texture is ranked only eighth among the criteria of the CART classification (Table SM4), and more importantly, the expert classification does not consider it, although the classification performs well for predicting infiltration rates. Similarly, Jarvis et al. (2013) reported that the hydraulic conductivity of topsoil was only weakly correlated with texture.

The third category of SSDs includes surface roughness and soil consolidation. The fact that these factors are not retained as discriminating factors by any of the classifications may be due to two reasons. One reason is that the information they convey is already conveyed by the criteria taken into account by the classifications. Soil consolidation and soil surface roughness are shown above to be correlated with the clod cover selected in both the expert and CART classifications. Another reason may be that they are weak proxies for the soil infiltration capacity. Especially, the role of soil surface roughness is generally considered complex and variable (e.g., Govers et al., 2000; Bahddou

et al., 2023).

Eventually, let us point out that in the expert and CART classifications we did not consider land use or soil type for discriminating between soil infiltration rates. We assumed that all SSDs describing the surface cover of the plots, for example, clods, soil crusts or vegetation covers, are better proxies of infiltration properties because they describe precisely the temporal changes in topsoil characteristics that can occur within a given land use type or soil type according to the timing of agricultural operations and climate and biological processes. To confirm this assumption, the CART approach was also applied by adding land use and FAO soil classes to the twelve SSDs. No significant improvement in the predicted percentage of variance (81 %) is identified compared with the CART classification based only on the twelve SSDs.

5.3. Operationality and limits of the proposed expert SSC classification

The expert classification can facilitate the identification of the SSC classes in the field and thereby the soil infiltration capacity of a given field. To that aim, a user has to observe at the field site the 5 criteria considered by the identification chart of the expert classification in Fig. 2. The criteria are easy and fast to observe by any operator after some training. They correspond only to soil cover variables, and their critical threshold values are simple and fixed at either 25 or 50 %, which facilitates field observations. Once the SSC class of the field is determined thanks to the identification chart, the soil infiltration capacity can be estimated by the mean class value of steady-state infiltration rates as given in Table 3.

In contrast to the expert-based classification, the statistically inferred SSC classification involves not only soil cover variables but also variables that require more measurement efforts (e.g., slope or soil texture) and defines very precise thresholds that cannot easily be discriminated in the field. Moreover, cross-validation reveals that the statistically inferred SSC classification is less precise and robust in predicting infiltration rates than the expert classification is. Indeed, the CART classification has to be calibrated and is thus sample dependent, whereas the expert classification is based on general knowledge about the relationships between infiltration capacity and SSCs in agricultural soils. However, there are some limits to the expert classification. First, the dataset used for evaluation includes pre-existing datasets collected at several sites in France and Tunisia, which leads to some imbalance in the number of observations for each land use, soil type or SSC class (Table 1). For example, observations for vineyards and wheat and barley, Calcisols and the SSC class VCst are numerous in the dataset, whereas observations on rangeland as well as on vertic Leptosols and on the SSC class VCsd are limited. Further evaluation including more plots belonging to the latter land uses, soil types and SSC classes that are insufficiently represented in our dataset would therefore be useful for confirming the relevance of the classification. Second, the actual performance of the expert classification in predicting topsoil infiltration rates depends not only on the SSC classification itself but also on the estimation of the mean infiltration rates per class. In this respect, the rainfall simulations only allow observations of infiltration rates up to 35 mm/h for application, which leads to underestimation of both the mean and range of variation in infiltration rates for the SSC classes with the highest infiltration rates. For those classes, additional rainfall simulations with larger rainfall rates are needed to estimate unbiased infiltration means. Finally, the expert classification does not consider the influence of soil compaction due to machinery traffic, tillage or cattle trampling on the SSCs, which may restrict the soil infiltration capacity. To this end, additional descriptors concerning soil compaction need to be taken into account. The qualitative observation of soil consolidation, as performed here by considering only two categories, weak and strong, is not sufficient to estimate the extent of soil compaction. However, this may not be a serious limitation in the context of the Mediterranean climate, because the risks of soil compaction are lower than those in more temperate regions given the shorter wet periods. Lagacherie et al.

Table 3

Estimated mean and standard deviation values of steady state infiltration rates per expert-based SSC class.

SSC class	T	TCst	Cst	VCst	LCst	Csd	VCsd	LCsd	S
Mean infiltration rate (mm/h)	33.7	26.2	16.5	31.6	27.6	7.5	8.2	13.8	28.4
Standard deviation (mm/h)	3	6.7	8	4.6	6.7	2.6	5.9	3.6	5.2

(2006) reported, for example, that Mediterranean vineyards regularly subjected to operations with heavy machinery (tillage, weeding, harvesting) exhibit only moderate soil compaction.

6. Conclusions

In this paper, we presented an expert-based classification of SSCs and evaluated it for predicting the steady infiltration rates of agricultural Mediterranean soils. The expert classification considers 9 SSC classes that are generic and can be identified in the field by an identification chart on the basis of five easy-to-observe SSDs, namely, the percentages of soil cover by clods, surface crusts, rock fragments, herbaceous vegetation and litter. Our results first show that the expert classification allowed us to discriminate infiltration rates between the 9 SSC classes with an RMSE of 5.2 mm/h, which is markedly more precise than the prediction of the saturated hydraulic conductivity of soils by current pedotransfer functions. Accordingly, our results confirmed our prior hypothesis that simple soil surface cover descriptors can be relevant and sufficient proxies to predict the infiltration capacity of agricultural soils. Considering additional criteria for classifying the SSCs by tree regression did not significantly improve the discrimination performance of the SSC classes for the soil infiltration rates. This study thus illustrates the paramount importance of using soil structure-related indicators or factors, such as the five SSDs considered by the expert classification, to achieve accurate estimations of soil hydraulic properties.

Finally, the benefits of the expert classification of SSC should be stressed. First, the classification provides an easy and accurate way to estimate the variation in soil infiltration capacity both between agricultural fields and with time in a given field according to soil treatments and changes in vegetation cover. It may therefore be useful for water management planning or hydrological modelling. Second, because the classification is based solely on soil surface descriptors, remote sensing approaches may be developed for their automatic recognition, which would facilitate their implementation for large areas. Examples of such approaches can be found in Corbane et al. (2008), Gao et al. (2020), and Gomez et al. (2022). Last, although the classification was initially derived and evaluated for Mediterranean agricultural soils, its concepts are general and could thus be tested and possibly adapted for agricultural soils in other climate and farming environments.

CRedit authorship contribution statement

Patrick Andrieux: Writing – review & editing, Writing – original draft, Visualization, Validation, Project administration, Methodology, Investigation, Funding acquisition, Formal analysis, Data curation, Conceptualization. **Marc Voltz:** Writing – review & editing, Writing – original draft, Visualization, Validation, Supervision, Methodology, Investigation, Formal analysis, Conceptualization. **Jean-Stéphane Bailly:** Writing – review & editing, Visualization, Validation, Methodology, Investigation, Formal analysis, Conceptualization. **Rafia Attia:** Resources, Investigation, Funding acquisition, Data curation. **Patrick Zante:** Methodology, Investigation, Data curation.

Declaration of competing interest

The authors declare that they have no known competing financial interests or personal relationships that could have appeared to influence the work reported in this paper.

Acknowledgements

This work is based on many rainfall simulations in France and Tunisia. We are therefore very much indebted to all those who contributed to the implementation and interpretation of the measurements at one or several of the study sites, namely, S. Agrebaoui, J. Asseline, B. Dridi, F. Gaddas, François Garnier, A. Hatier, J. Leonard, I. Marques, and Gwenn Trotoux. We are also grateful to G. Coulouma for assisting in the identification of WRB soil classes and advice on the present manuscript, D. Cornet for assisting in preliminary statistical analyses and D. Raclot for facilitating observations at the Kamech site in Tunisia. We thank the second reviewer of the paper for his comments that helped to improve the manuscript. Finally, we would like to acknowledge J.L. Belotti and Zakia Jenhaoui for their monitoring of the soil surface conditions at the OMERE long-term observatories, which has played a key role in the development of expert classification of the surface conditions of Mediterranean soils.

Appendix A. Supplementary data

Supplementary data to this article can be found online at <https://doi.org/10.1016/j.geoderma.2025.117468>.

Data availability

The authors do not have permission to share data.

References

- AFNOR, 2003. NF X 31-107 Soil Quality—Particle Size Determination by Sedimentation—Pipette Method. AFNOR Editions, La Plaine Saint-Denis, France.
- Aguilera, H., Guardiola-Albert, C., Moreno Merino, L., Baquedano, C., Díaz-Losada, E., Robledo Ardila, P.A., Duran Valsero, J.J., 2022. Building inexpensive topsoil saturated hydraulic conductivity maps for land planning based on machine learning and geostatistics. *Catena* 208, 105788. <https://doi.org/10.1016/j.catena.2021.105788>.
- Andrieux, P., Coulouma, G., Zante, P., Belotti, J.L., Garnier, F., Huttel, O., Negro, S., Pepin, Y., Richard, J., 2007. Impact de techniques culturales sur le ruissellement, l'érosion et la structure des sols viticoles. Rapport final, 12ème Contrat Etat Région, « Pérennité des sols viticoles, itinéraires culturaux et activités biologiques des sols ». UMR LISAH, Montpellier, 41 pp.
- Arnau-Rosalén, E., Calvo-Cases, A., Boix-Fayos, C., Lavee, H., Sarah, P., 2008. Analysis of soil surface component patterns affecting runoff generation. An example of methods applied to Mediterranean hillslopes in Alicante (Spain). *Geomorphology* 101, 595–606. <https://doi.org/10.1016/j.geomorph.2008.03.001>.
- Asseline, J., Valentin, C., 1978. Construction et mise au point d'un infiltromètre à aspersion. *Les Cahiers De l'ORSTOM, Série Hydrologie* 15, 321–349. <http://pascal-francis.inist.fr/vibad/index.php?action=getRecordDetail&idt=12716013>.
- Assouline, S., 2004. Rainfall-induced soil surface sealing: a critical review of observations, conceptual models, and solutions. *Vadose Zone J.* 3, 570–591. <https://doi.org/10.2136/vzj2004.0570>.
- Attia, R., Zante, P., Andrieux, P., Agrebaoui, S., Dridi, B., Hamrouni, H., Touma, J., 2009. Evolution et caractérisation hydrodynamique des états de surface. Bassin versant de El Hnach (Tunisie). Rapport UMR LISAH et DG ACTA-Direction des Sols Tunis, 44 pp.
- Bahddou, S., Otten, W.S., Whalley, W.R., Shin, H.-C., El Gharous, M., Rickson, R.J., 2023. Changes in soil surface properties under simulated rainfall and the effect of surface roughness on runoff, infiltration and soil loss. *Geoderma* 431, 116341. <https://doi.org/10.1016/j.geoderma.2023.116341>.
- Bargués-Tobella, A., Winowiecki, L.A., Sheil, D., Vågen, T.-G., 2024. Determinants of field-saturated soil hydraulic conductivity across sub-Saharan Africa: texture and beyond. *Water Resour. Res.* 60, e2023WR035510. <https://doi.org/10.1016/j.geoderma.2023.116341>.
- Berndtsson, R., Larson, M., 1987. Spatial variability of infiltration in a semi-arid environment. *J. Hydrol.* 90, 117–133. [https://doi.org/10.1016/0022-1694\(87\)90175-2](https://doi.org/10.1016/0022-1694(87)90175-2).

- Biarnes, A., Rio, P., Hocheux, A., 2004. Analyzing the determinants of spatial distribution of weed control practices in a Languedoc vineyard catchment. *Agronomie* 24, 187–196. <https://doi.org/10.1051/agro:2004018>.
- Blanchy, G., Albrecht, L., Bragato, G., Garré, S., Jarvis, N., Koestel, J., 2023. Impacts of soil management and climate on saturated and near-saturated hydraulic conductivity: analyses of the Open Tension-disk Infiltrometer Meta-database (OTIM). *Hydrol. Earth Syst. Sci.* 27, 2703–2724. <https://doi.org/10.5194/hess-27-2703-2023>.
- Bresson, L.M., Boiffin, J., 1990. Morphological characterization of soil crust development stages on an experimental field. *Geoderma* 47, 301–325. [https://doi.org/10.1016/0016-7061\(90\)90035-8](https://doi.org/10.1016/0016-7061(90)90035-8).
- Boiffin, J., 1984. La dégradation structurale des couches superficielles du sol sous l'action des pluies. Sciences agronomiques. Ph.D. Thesis. INA P-G, Paris, 320 pp.
- Boiffin, J., Papy, F., Eimberck, J., 1988. Influence des systèmes de culture sur les risques d'érosion par ruissellement concentré. I. Analyse des conditions de déclenchement de l'érosion. *Agronomie* 8, 663–673. <https://hal.archives-ouvertes.fr/hal-00885148>.
- Bormann, H., 2010. Towards a hydrologically motivated soil texture classification. *Geoderma* 157, 142–153. <https://doi.org/10.1016/j.geoderma.2010.04.005>.
- Breiman, L., Friedman, J.H., Olshen, R.A., Stone, C.J., 1984. *Classification And Regression Trees* (1st ed.). Routledge, New York. <https://doi.org/10.1201/9781315139470>.
- Casenave, A., Valentin, C., 1992. A runoff capability classification system based on surface features criteria in semi-arid areas of West Africa. *J. Hydrol.* 130, 231–249. [https://doi.org/10.1016/0022-1694\(92\)90112-9](https://doi.org/10.1016/0022-1694(92)90112-9).
- Cerdà, A., 2001. Effects of rock fragment cover on soil infiltration, interrill runoff and erosion. *Eur. J. Soil Sci.* 52, 59–68. <https://doi.org/10.1046/j.1365-2389.2001.00354.x>.
- Cerdan, O., Souchère, V., Lecomte, V., Couturier, A., Le Bissonnais, Y., 2001. Incorporating soil surface crusting processes in an expert-based runoff and erosion model: STREAM (sealing and transfer by runoff and erosion related to agricultural management). *Catena* 46, 189–205. [https://doi.org/10.1016/S0341-8162\(01\)00166-7](https://doi.org/10.1016/S0341-8162(01)00166-7).
- Chahinian, N., Moussa, R., Andrieux, P., Voltz, M., 2006a. Accounting for temporal variation in soil hydrological properties when simulating surface runoff on tilled plots. *J. Hydrol.* 326, 135–152. <https://doi.org/10.1016/j.jhydrol.2005.10.038>.
- Chahinian, N., Voltz, M., Moussa, R., Trotoux, G., 2006b. Assessing the impact of the hydraulic properties of a crusted soil on overland flow modelling at the field scale. *Hydrol. Process.* 20, 1701–1722. <https://doi.org/10.1002/HYP.5948>.
- Clapp, R.B., Hornberger, G.M., 1978. Empirical equations for some soil hydraulic properties. *Water Resour. Res.* 14, 601–604. <https://doi.org/10.1029/WR014i004p0601>.
- Corbane, C., Raclot, D., Jacob, F., Albergel, J., Andrieux, P., 2008. Remote sensing of soil surface characteristics from a multiscale classification approach. *Catena* 75, 308–318. <https://doi.org/10.1016/j.catena.2008.07.009>.
- Cosby, B.J., Hornberger, G.M., Clapp, R.B., Ginn, T.R., 1984. A statistical exploration of the relationships of soil moisture characteristics to the physical properties of soils. *Water Resour. Res.* 20, 682–690. <https://doi.org/10.1029/WR020i006p0682>.
- Descroix, L., Viramontes, D., Gonzalez-Barrios, J.L., Vauclin, M., Esteves, M., 2001. Influence of soil surface feature and vegetation on runoff and erosion in the Western Sierra Madre (Durango Northwest Mexico). *Catena* 43, 115–135. [https://doi.org/10.1016/S0341-8162\(00\)00124-7](https://doi.org/10.1016/S0341-8162(00)00124-7).
- Essig, E.T., Corradini, C., Morbidelli, R., Govindaraju, R.S., 2009. Infiltration and deep flow over sloping surfaces: comparison of numerical and experimental results. *J. Hydrol.* 374, 30–42. <https://doi.org/10.1016/j.jhydrol.2009.05.017>.
- European Environment Agency, 2012. The major soil types of Europe. European Union. <https://www.eea.europa.eu/data-and-maps/figures/the-major-soil-types-of-europe>.
- European Soils Bureau Network, 2005. Soil atlas of Europe. European Commission, Office for official publications of the European Communities, L-2995 Luxembourg, pp. 86–91. <https://esdac.jrc.ec.europa.eu/content/soil-atlas-europe>.
- FAO (Ed.), 2006. Guidelines for soil description (4th ed.). Rome, Italy. https://www.researchgate.net/publication/40106751_FAO_Guidelines_for_Soil_Description.
- Gao, L., Wang, X., Johnson, B.A., Tian, Q., Wang, Y., Verrelst, J., Mu, X., Gu, X., 2020. Remote sensing algorithms for estimation of fractional vegetation cover using pure vegetation index values: a review. *ISPRS J. Photogramm. Remote Sens.* 159, 364–377. <https://doi.org/10.1016/j.isprsjprs.2019.11.018>.
- Gicheru, P., Gachene, C., Mbuvi, J., Mare, E., 2004. Effects of soil management practices and tillage systems on surface soil water conservation and crust formation on a sandy loam in semi-arid Kenya. *Soil & Tillage Res.* 75, 173–184. [https://doi.org/10.1016/S0167-1987\(03\)00161-2](https://doi.org/10.1016/S0167-1987(03)00161-2).
- Gomez, C., Aboubacar, M.S., Ienco, D., Feurer, D., Jenhaoui, Z., Rafla, A., Teisseire, M., Bailly, J.S., 2022. Sentinel-2 images to assess soil surface characteristics over a rainfed Mediterranean cropping system. *Catena* 213. <https://doi.org/10.1016/j.catena.2022.106152>.
- Govers, G., Takken, I., Helming, K., 2000. Soil roughness and overland flow. *Agronomie* 20, 131–146. <https://hal.archives-ouvertes.fr/hal-00885998>.
- Groenendyk, D.G., Ferré, T.P.A., Thorp, K.R., Rice, A.K., 2015. Hydrologic-process-based soil texture classifications for improved visualization of landscape function. *PLoS One* 10, e0131299. <https://doi.org/10.1371/journal.pone.0131299>.
- Gupta, S., Hengl, T., Lehmann, P., Bonetti, S., Or, D., 2021. SoilKsatDB: global database of soil saturated hydraulic conductivity measurements for geoscience applications. *Earth Syst. Sci. Data* 13, 1593–1612. <https://doi.org/10.5194/essd-13-1593-2021>.
- Gyssels, G., Poesen, J., 2003. The importance of plant root characteristics in controlling concentrated flow erosion rates. *Earth Surf. Process. Landforms* 28, 371–384. <https://doi.org/10.1002/esp.447>.
- Hastie, T., Tibshirani, R., Friedman, J., 2001. *The Elements of Statistical Learning*. Springer, New York.
- IUSS Working Group WRB, 2015. World Reference Base for Soil Resources 2014, update 2015 International soil classification system for naming soils and creating legends for soil maps. World Soil Resources Reports No. 106. FAO, Rome.
- Janeau, J.L., Bricquet, J.P., Planchon, O., Valentin, C., 2003. Soil erosion and infiltration on very steep slopes in northern Thailand. *Eur. J. Soil Sci.* 5, 543–553. <https://doi.org/10.1046/j.1365-2389.2003.00494.x>.
- Jarvis, N., Koestel, J., Messing, I., Moeys, J., Lindahl, A., 2013. Influence of soil, land use and climatic factors on the hydraulic conductivity of soil. *Hydrol. Earth System Sci.* 17, 5185–5195. <https://doi.org/10.5194/hess-17-5185-2013>.
- Jorda, H., Bechtold, M., Jarvis, N., Koestel, J., 2015. Using boosted regression trees to explore key factors controlling saturated and near-saturated hydraulic conductivity. *Eur. J. Soil Sci.* 66, 744–756. <https://doi.org/10.1111/ejss.12249>.
- Lagacherie, P., Coulouma, G., Ariagno, P., Virat, P., Boizard, H., Richard, G., 2006. Spatial variability of soil compaction over a vineyard region in relation with soils and cultivation operations. *Geoderma* 134, 207–216. <https://doi.org/10.1016/j.geoderma.2005.10.006>.
- Lagacherie, P., Alvaro-Fuentes, J., Annabi, M., Bernoux, M., Bouarfia, S., Douaoui, A., Grunberger, O., Hammani, A., Montanarella, L., Mrabet, R., Sabir, M., Raclot, D., 2018. Managing Mediterranean soil resources under global change: expected trends and mitigation strategies. *Reg. Environ. Chang.* 18, 663–675. <https://doi.org/10.1007/s10113-017-1239-9>.
- Le Bissonnais, Y., Cerdan, O., Lecomte, V., Benkhadra, H., Souchère, V., Martin, P., 2005. Variability of soil surface characteristics influencing runoff and interrill erosion. *Catena* 62, 111–124. <https://doi.org/10.1016/j.catena.2005.05.001>.
- Leonard, J., Andrieux, P., 1998. Infiltration characteristics of soils in Mediterranean vineyards in southern France. *Catena* 32, 209–223. [https://doi.org/10.1016/S0341-8162\(98\)00049-6](https://doi.org/10.1016/S0341-8162(98)00049-6).
- Lu, J., Zhang, Q., Werner, A.D., Li, Y., Jiang, S., Tan, Z., 2020. Root-including changes of soil hydraulic properties—a review. *J. Hydrol.* 589, 125203. <https://doi.org/10.1016/j.jhydrol.2020.125203>.
- Ludwig, B., Boiffin, J., Chadoeuf, J., Auzet, A.V., 1995. Hydrological structure and erosion damage caused by concentrated flow in cultivated catchments. *Catena* 25, 227–252. [https://doi.org/10.1016/0341-8162\(95\)00012-H](https://doi.org/10.1016/0341-8162(95)00012-H).
- Malet, J.P., Auzet, A.V., Maquaire, O., Ambroise, B., Descroix, L., Esteves, M., Vandervaere, J.P., Truchet, E., 2003. Soil surface characteristics influence on infiltration in black marls: application to the Super-Sauze earthflow (southern Alps, France). *Earth Surf. Process. Landforms* 28, 547–564. <https://doi.org/10.1002/esp.457>.
- Martínez-Zavala, L., Jordán, A., A., 2008. Effect of rock fragment cover on interrill soil erosion from bare soils in Western Andalusia Spain. *Soil Use Manag.* 24, 108–117. <https://doi.org/10.1111/j.1475-2743.2007.00139.x>.
- Morbidegli, R., Saltalippi, C., Flammini, A., Govindaraju, R.S., 2018. Role of slope on infiltration: a review. *J. Hydrol.* 557, 878–886. <https://doi.org/10.1016/j.jhydrol.2018.01.019>.
- Morvan, X., Naisse, C., Malam Issa, O., Desprats, J.F., Combaud, A., Cerdan, O., 2014. Effect of ground-cover type on surface runoff and subsequent soil erosion in Champagne vineyards in France. *Soil Use Manag.* 30, 372–381. <https://doi.org/10.1111/sum.12129>.
- Mwendera, E.J., Feyen, J., 1994. Effects of tillage and rainfall on soil surface roughness and properties. *Soil Technol.* 7, 93–103. [https://doi.org/10.1016/0933-3630\(94\)90010-8](https://doi.org/10.1016/0933-3630(94)90010-8).
- Neave, M., Rayburg, S., 2007. A field investigation into the effects of progressive rainfall-induced soil seal and crust development on runoff and erosion rates: the impact of surface cover. *Geomorphology* 87, 378–390. <https://doi.org/10.1016/j.geomorph.2006.10.007>.
- Ottoni, M.V., Ottoni Filho, T.B., Lopes-Assad, M.L.R., Rotunno Filho, O.C., 2019. Pedotransfer functions for saturated hydraulic conductivity using a database with temperate and tropical climate soils. *J. Hydrol.* 575, 1345–1358. <https://doi.org/10.1016/j.jhydrol.2019.05.050>.
- Parasuraman, K., Elshorbagy, A., Si, B.C., 2006. Estimating saturated hydraulic conductivity in spatially variable fields using neural network ensembles. *Soil Sci. Soc. Am. J.* 70, 1851–1859. <https://doi.org/10.2136/sssaj2006.0045>.
- Pare, N., Andrieux, P., Louchart, X., Biarnes, A., Voltz, M., 2011. Predicting the spatio-temporal dynamic of soil surface characteristics after tillage. *Soil & Tillage Res.* 114, 135–145. <https://doi.org/10.1016/j.still.2011.04.003>.
- Pham, K., Won, J., 2022. Enhancing the tree-boosting-based pedotransfer function for saturated hydraulic conductivity using data preprocessing and predictor importance using game theory. *Geoderma* 420, 115864. <https://doi.org/10.1016/j.geoderma.2022.115864>.
- Poesen, J., Lavee, H., 1994. Rock fragments in top soils: significance and processes. *Catena* 23, 1–28. [https://doi.org/10.1016/0341-8162\(94\)90050-7](https://doi.org/10.1016/0341-8162(94)90050-7).
- Poesen, J., Ingelmo-Sanchez, F., Múcher, H., 1990. The hydrological response of soil surfaces to rainfall as affected by cover and position of rock fragments in the top layer. *Earth Surf. Process. Landforms* 15, 653–671. <https://doi.org/10.1002/esp.3290150707>.
- Rahmati, M., Weiermüller, L., Vanderborcht, J., Pachepsky, Y.A., Mao, L., Sadeghi, S.H., Moosavi, N., Kheirfam, H., Montzka, C., Van Looy, K., Toth, B., Hazbavi, Z., Al Yamani, W., Albalasmeh, A.A., Alghzawi, M.Z., Angulo-Jaramillo, R., Antonino, A.C.D., Arampatzis, G., Armindo, R.A., Asadi, H., Bamutaze, Y., Batlle-Aguilar, J., Béchet, B., Becker, F., Blöschl, G., Bohne, K., Braud, I., Castellano, C., Cerdà, A., Chalhouh, M., Cichota, R., Císlarová, M., Clothier, B., Coquet, Y., Cornelis, W., Corradini, C., Coutinho, A.P., de Oliveira, M.B., de Macedo, J.R., Durães, M.F., Emami, H., Eskandari, I., Farajnia, A., Flammini, A., Fodor, N., Gharibeh, M., Ghavimipanh, M.H., Ghezzehei, T.A., Giertzi, S., Hatzigiannakis, E.G., Horn, R., Jiménez, J.J., Jacques, D., Keesstra, S.D., Kelishadi, H., Kiani-Harchegani, M., Kouselou, M., Kumar Jha, M., Lassabatere, L., Li, X., Liebig, M.A., Lichner, L.,

- López, M.V., Machiwal, D., Mallants, D., Mallmann, M.S., de Oliveira Marques, J.D., Marshall, M.R., Mertens, J., Meunier, F., Mohammadi, M.H., Mohanty, B.P., Pulido-Moncada, M., Montenegro, S., Morbidelli, R., Moret-Fernández, D., Moosavi, A.A., Mosaddeghi, M.R., Mousavi, S.B., Mozaffari, H., Nabiollahi, K., Neyshabouri, M.R., Ottoni, M.V., Ottoni Filho, T.B., Pahlavan-Rad, M.R., Panagopoulos, A., Peth, S., Peyneau, P.-E., Picciafuoco, T., Poesen, J., Pulido, M., Reinert, D.J., Reinsch, S., Rezaei, M., Roberts, F.P., Robinson, D., Rodrigo-Comino, J., Rotunno Filho, O.C., Saito, T., Saganuma, H., Saltalippi, C., Sándor, R., Schütt, B., Seeger, M., Sepehrnia, N., Sharifi Moghaddam, E., Shukla, M., Shutaro, S., Sorando, R., Stanley, A.A., Strauss, P., Su, Z., Taghizadeh-Mehrjardi, R., Taguas, E., Teixeira, W. G., Vaezi, A.R., Vafakhah, M., Vogel, T., Vogeler, I., Votrubova, J., Werner, S., Winarski, T., Yilmaz, D., Young, M.H., Zacharias, S., Zeng, Y., Zhao, Y., Zhao, H., Vereecken, H., 2018. Development and analysis of the soil water infiltration global database. *Earth Syst. Sci. Data* 10, 1237–1263. <https://doi.org/10.5194/essd-10-1237-2018>.
- Roth, C.H., 2004. A framework relating soil surface condition to infiltration and sediment and nutrient mobilization in grazed rangelands of Northeastern Queensland Australia. *Earth Surf. Process. Landforms* 29, 1093–1104. <https://doi.org/10.1002/esp.1104>.
- Ruiz Sinoga, J.D., Diaz, A.R., Bueno, E.F., Murillo, J.F.M., 2010. The role of soil surface conditions in regulating runoff and erosion processes on a metamorphic hillslope (Southern Spain) Soil surface conditions, runoff and erosion in Southern Spain. *Catena* 80, 131–139. <https://doi.org/10.1016/j.catena.2009.09.007>.
- Sandin, M., Jarvis, N., Larsbo, M., 2018. Consolidation and surface sealing of nine harrowed Swedish soils. *Soil & Tillage Res.* 181, 82–92. <https://doi.org/10.1016/j.still.2018.03.017>.
- Saxton, K.E., Rawls, W., Romberger, J.S., Papendick, R.I., 1986. Estimating generalized soil-water characteristics from texture. *Soil Sci. Soc. Am. J.* 50, 1031–1036. <https://doi.org/10.2136/sssaj1986.03615995005000040039x>.
- Schaap, M.G., Leij, F.J., van Genuchten, M.T., 2001. ROSETTA: a computer program for estimating soil hydraulic parameters with hierarchical pedotransfer functions. *J. Hydrol.* 251, 163–176. [https://doi.org/10.1016/S0022-1694\(01\)00466-8](https://doi.org/10.1016/S0022-1694(01)00466-8).
- Shao, Q., Baumgartl, T., 2014. Estimating input parameters for four infiltration models from basic soil, vegetation, and rainfall properties. *Soil Sci. Soc. Am. J.* 78, 1507–1521. <https://doi.org/10.2136/sssaj2014.04.0122>.
- Therneau, T., Atkinson, B., Ripley, B., 2013. Rpart: recursive partitioning. R Package Version 4.1-3. <http://cran.r-project.org/package=rpart>.
- Thompson, S.E., Harman, C.J., Heine, P., Katul, G.G., 2010. Vegetation-infiltration relationships across climatic and soil type gradients. *J. Geophys. Res.* 115, G02023. <https://doi.org/10.1029/2009JG001134>.
- Tighe, M., Muñoz-Robles, C., Reid, N., Wilson, B., Briggs, S.V., 2012. Hydrological thresholds of soil surface properties identified using conditional inference tree analysis. *Earth Surf. Process. Landforms* 37, 620–632. <https://doi.org/10.1002/esp.3191>.
- Tongway, D.J., Hindley, N.L., 1995. *Manual for Assessment of Soil Condition of Tropical Grasslands*. CSIRO Division of Wildlife & Ecology, Canberra.
- Tóth, B., Weynants, M., Pásztor, L., Hengl, T., 2017. 3D soil hydraulic database of Europe at 250 m resolution. *Hydrol. Process.* 31, 2662–2666. <https://doi.org/10.1002/hyp.11203>.
- Valentin, C., Bresson, L.M., 1992. Morphology, genesis and classification of surface crusts in loamy and sandy soils. *Geoderma* 55, 225–245. [https://doi.org/10.1016/0016-7061\(92\)90085-L](https://doi.org/10.1016/0016-7061(92)90085-L).
- Van Looy, K., Bouma, J., Herbst, M., Koestel, J., Minasny, B., Mishra, U., Vereecken, H., 2017. Pedotransfer functions in Earth system science: challenges and perspectives. *Reviews Geophys.* 55, 1199–1256. <https://doi.org/10.1002/2017RG000581>.
- Vereecken, H., Maes, J., Feyen, J., 1990. Estimating unsaturated hydraulic conductivity from easily measured soil properties. *Soil Sci.* 149, 1–12. <https://doi.org/10.1097/00010694-199001000-00001>.
- Vereecken, H., Weiermüller, L., Assouline, S., Šimůnek, J., Verhoef, A., Herbst, M., Archer, N., Mohanty, B., Montzka, C., Vanderborght, J., Balsamo, G., Bechtold, M., Boone, A., Chadburn, S., Cuntz, M., Decharme, B., Ducharne, A., Ek, M., Garrigues, S., Goergen, K., Ingwersen, J., Kollet, S., Lawrence, D.M., Li, Q., Or, D., Swenson, S., de Vrese, P., Walko, R., Wu, Y., Xue, Y., 2019. Infiltration from the pedon to global grid scales: an overview and out-look for land surface modeling. *Vadose Zone J.* 18, 180191. <https://doi.org/10.2136/vzj2018.10.019>.
- Voltz, M., Ludwig, W., Leduc, C., Bouarfa, S., 2018. Mediterranean land surfaces under global change: current state and future challenges. *Reg. Environ. Chang.* 18, 619–622. <https://doi.org/10.1007/s10113-018-1295-9>.
- Wang, L., Zhang, G., Zhu, P., Wang, X., 2020. Comparison of the effects of litter covering and incorporation on infiltration and soil erosion under simulated rainfall. *Hydrol. Process.* 34, 2911–2922. <https://doi.org/10.1002/hyp.13779>.
- Wösten, J.H.M., Lilly, A., Nemes, A., Le Bas, C., 1999. Development and use of a database of hydraulic properties of European soils. *Geoderma* 90, 169–185. [https://doi.org/10.1016/S0016-7061\(98\)00132-3](https://doi.org/10.1016/S0016-7061(98)00132-3).
- Yang, J.L., Zhang, G.L., Yang, F., Yang, R.M., Yi, C., Li, D., Zhao, Y.G., Liu, F., 2016. Controlling effects of surface crusts on water infiltration in an arid desert area of Northwest China. *J. Soil. Sediment.* 16, 2408–2418. <https://doi.org/10.1007/s11368-016-1436-z>.
- Zante, P., Attia, R., Andrieux, P., Agrebaoui, S., Dridi, B., Hamrouni, H., Lamachere, J.M., Touma, J., 2007. Evolution et caractérisation hydrodynamique des états de surface. Bassin versant de El Gouazine (Tunisie). Rapport UMR LISAH, Montpellier et DG ACTA-Direction des Sols, Tunis, 45 pages.
- Zante, P., Andrieux, P., Attia, R., Hamrouni, H., Raclot, D., Touma, J., Agrebaoui, S., Dridi, B., 2009. Caractérisation hydrodynamique des états de surface: bassin versant de Kamech (Tunisie). Rapport UMR LISAH, Montpellier et DG ACTA-Direction des Sols, Tunis, 41 pages.
- Zhang, Y., Schaap, M.G., 2017. Weighted recalibration of the Rosetta pedotransfer model with improved estimates of hydraulic parameter distributions and summary statistics (Rosetta3). *J. Hydrol.* 547, 39–53. <https://doi.org/10.1016/j.jhydrol.2017.01.004>.
- Zhang, X., Zhu, J., Wendroth, O., Matocha, C., 2019. Effect of macroporosity on pedotransfer function estimates at the field scale. *Vadose Zone J.* 18, 180151. <https://doi.org/10.2136/vzj2018.08.0151>.
- Zhipeng, L., Donghao, Ma., Wei, Hu., Xuelin, L.i., 2018. Land use dependent variation of soil water infiltration characteristics and their scale-specific controls. *Soil & Tillage Res.* 178, 139–149. <https://doi.org/10.1016/j.still.2018.01.001>.
- Zi, R., Han, Z., Chen, T., Fang, F., Fang, Q., Peng, L., Qian, X., Yin, X., Zhao, L., 2024. Quantifying the effects of rock fragments embedding vs covering on soil erosion in karst sloping cropland. *Catena* 244, 108234. <https://doi.org/10.1016/j.catena.2024.108234>.